UM–TH–96–13
hep-ph/9609210

Searching for a Light Stop at the Tevatron

Gregory Mahlon* and G.L. Kane†

Department of Physics, University of Michigan

500 E. University Ave., Ann Arbor, MI 48109

(August 30, 1996)

Abstract

We describe a method to help the search for a light stop squark ($\widetilde{M}_t + \widetilde{M}_{LSP} < m_t$) at the Fermilab Tevatron. Traditional search methods rely upon a series of stringent background-reducing cuts which, unfortunately, leave very few signal events given the present data set. To avoid this difficulty, we instead suggest using a milder set of cuts, combined with a "superweight," whose purpose is to discriminate between signal and background events. The superweight consists of a sum of terms, each of which are either zero or one. The terms are assigned event-by-event depending upon the values of various observables. We suggest a method for choosing the observables as well as the criteria used to assign the values such that the superweight is "large" for the supersymmetric signal and "small" for the standard model background. For illustration, we mainly consider the detection of stops coming from top decay, making our analysis especially relevant to the W + 2 jets top sample.

14.80.Ly, 12.60.Jv, 14.65.Ha

I. INTRODUCTION

There has been recent activity in the area of weak-scale supersymmetry, spurred on by a number of suggestive experimental results. First, there is the single $ee\gamma\gamma + \not{E}_T$ event observed by CDF [1]. This particular event does not seem to have a Standard Model interpretation. Also, in supersymmetry, the $Z \to b\bar{b}$ rate ($R_b = \Gamma(Z \to b\bar{b})/\Gamma(Z \to \text{hadrons})$), the value of α_s extracted from Γ_Z, and the branching ratio for $b \to s\gamma$ are all affected by loop diagrams containing charginos and stop squarks. At present [2], all three of these quantities are 1.5–2.0σ from their Standard Model predictions, each in precisely the directions expected from supersymmetry [2–7] if there is a light stop squark.

Remarkably, these experimentally independent "mysteries" can all be explained by a single reasonably well-determined set of parameters within the framework of weak scale supersymmetry. The $ee\gamma\gamma + \not{E}_T$ event has a natural interpretation in terms of selectron pair production. Two different scenarios are possible, depending upon whether the lightest supersymmetric particle (LSP) is a gravitino [8,9] or Higgsino-like neutralino [8]. The neutralino and chargino parameters suggested by the second scenario overlap with the values required to account for the R_b difference [4], provided that one of the stop squark eigenstates is light ($\widetilde{M}_t \lesssim m_W$).

One might be concerned that such a low stop mass would have undesirable side-effects. Indeed, an immediate consequence [5] is that the decays

$$t \to \tilde{t} N_i \tag{1.1}$$

where $\tilde{t}$ is the lighter of the two stop mass eigenstates and N_i is a kinematically accessible neutralino mass eigenstate should occur with a total branching ratio in the neighborhood of 50%. The consequences of this depend on how the stop decays. When at least one chargino is light enough, the decay

$$\tilde{t} \to C_i b \tag{1.2}$$

dominates [10]. In this case, the subsequent chargino decay to a fermion-antifermion pair

plus neutralino leads to a $N_1 N_1 f \bar{f}' b$ final state whenever a top undergoes the decay (1.1). Since the final state for the SM decay is identical except for the (invisible) neutralinos, there is potential for both direct stop decays as well as top to stop decays to mimic ordinary top decays. This possibility has been investigated by several authors [10–14]. In particular, we note that Sender [14] finds that models with a "large" $\mathcal{B}(t \to \tilde{t} N_1)$ have not been ruled out by Tevatron data, provided the stop decays according to (1.2). This scenario, although interesting, is not the focus of this paper. Instead, we wish to examine the situation where the one-loop decay

$$\tilde{t} \to N_1 c \tag{1.3}$$

dominates, which happens when the decay (1.2) is kinematically forbidden [15]. In this case, a top undergoing the decay (1.1) would produce a $c N_1 N_1$ final state and be effectively invisible to standard searches. Two independent analyses appropriate to this case have been performed [14,16] which conclude that $\mathcal{B}(t \to X)$ where $X \neq Wb$ is at most 20–25%. However, neither analysis accounts for the possibility that supersymmetry can lead to additional sources of top quarks, without the need for stop decays masquerading as top decays [17]. For example, if the gluino is lighter than the other (non-stop) squark flavors, but heavier than $m_t + \widetilde{M}_t$, then it decays exclusively via [10]

$$\tilde{g} \to t\tilde{t}^-, \bar{t}\tilde{t}^+, \tag{1.4}$$

making the production of gluinos a source of top quarks [17,18]. In fact, the authors of Ref. [17] argue that there is indirect evidence for the decays (1.1), (1.3), and (1.4) in the Fermilab data on top rates and distributions.

In light of the indirect hints at weak scale supersymmetry, it is important to take every opportunity to obtain some direct evidence that nature is indeed supersymmetric, or, to show that it is not. A discussion of search strategies for the direct production of stop pairs at the Tevatron already exists in the literature [11]. The authors of Ref. [11] claim that a stop squark with a mass of up to about 100 GeV should be visible at the Tevatron in the

≥ 2 jets plus missing transverse energy channel given 100 pb^{-1} of data. Nevertheless, we feel that it is beneficial to augment the direct search with a search for stops coming from top decay: observation of a signal in both channels would greatly boost the case for SUSY. To this end, we present a method that may facilitate the search for top to stop decay at the Fermilab Tevatron. Our method consists of defining a superweight $\widetilde{\mathcal{X}}$ whose function is to discriminate between signal and background events. The superweight is constructed from various observables in the events so that it is "large" for the signal events and "small" for the background. We will illustrate the superweight method using the case of the stops coming from top quark decays; it can also be applied to stop pair production. Although the required analysis is not easy, it should be possible to determine directly whether about half of all tops indeed decay to stops. Our goal in this paper is to help this process.

The authors of Ref. [16] have also looked at the problem of searching for stops from top decay at the Tevatron. However, they employ the traditional method of cutting only on the kinematic observables in the event. As a result, their signal efficiencies are rather low (6%–8%). Also, they do not include the possibility of SUSY-induced $t\bar{t}$ production. Consequently, they conclude the prospects for observing a signal, if present, are most promising at an *upgraded* Tevatron. As we shall see, the superweight method allows us to reduce the backgrounds to a level similar to that of Ref. [16], but with efficiencies as high as 16%, providing for the possibility of finding a signal in the *current* data set.

The D0 experiment at Fermilab as well as the various LEP experiments have reported limits based upon searches for the pair production of stop squarks [19,20] (see Fig. 1). In the event that the current run at LEP finds a stop signal, the confirmation process could be greatly aided by the Tevatron data, depending upon the stop and LSP masses. On the other hand, even if LEP sees nothing, there is still a significant region in the stop-LSP mass plane to which the Tevatron is sensitive and which will not have been excluded by LEP.

The remainder of the paper is organized as follows: in Sec. II we briefly examine the generic features of SUSY models hinted at by the data, and determine the experimental signature we will concentrate on. Sec. III contains a general discussion of the superweight

and the methods by which it is constructed. We discuss the detection of the decay $t \to \tilde{t} N_1$ in Sec. IV, within the framework of a simplified model where no other neutralinos are light enough to be produced, and where only SM $t\bar{t}$ production mechanisms are considered. Such an analysis is appropriate for any SUSY model which contains the decays (1.1) and (1.3), whether or not there are extra sources of top quarks. We expand our discussion to include the other neutralinos and SUSY $t\bar{t}$ production mechanisms in Sec. V. Finally, Sec. VI contains our conclusions; Fig. 10 summarizes our results.

II. STOPS FROM TOP DECAY

A. A SUSY Model

In this section we flesh-out the supersymmetric scenario described in the introduction. Specifically, the picture implied by Refs. [4,8,17] contains a Higgsino-like neutralino N_1 with a mass in the 30 to 55 GeV range, a light stop squark with a mass in the 45 to 90 GeV range, a gluino with a mass in the 210 to 250 GeV range, and $\tilde{u}, \tilde{d}, \tilde{s}, \tilde{c}$ squarks in the 225 to 275 GeV range. The "heavy" stop eigenstate as well as both $\tilde{b}$ squark eigenstates may be heavier. We further assume that the "light" stop eigenstate is lighter than the charginos, and that the gluino is lighter than the squarks (except for $\tilde{t}$). The stop and the lighter chargino could be approximately degenerate; we ignore such a complication here. We take the top quark mass to be 163 GeV.

With these masses and couplings, the decays and branching ratios relevant to our study are

$$\mathcal{B}(\tilde{q} \to q\tilde{g}) \sim 25\%\text{–}75\% \tag{2.1}$$

$$\mathcal{B}(\tilde{g} \to t\tilde{t}^-) = \mathcal{B}(\tilde{g} \to \bar{t}\,\tilde{t}^+) = 50\% \tag{2.2}$$

$$\mathcal{B}(t \to Wb) \sim \mathcal{B}(t \to \tilde{t} N_i) \sim 50\% \tag{2.3}$$

$$\mathcal{B}(\tilde{t} \to cN_1) \sim 100\%. \tag{2.4}$$

The large variation in the branching ratio for squark decays is a consequence of the relatively small phase space available for producing gluinos; hence, 2-body decays to the electroweak superpartners are able to compete effectively with the strong decays. The gluinos, however, have no other 2-body decay modes: if top-stop is open, it dominates.

As indicated by (2.3), the total branching ratio for top to all of the kinematically accessible neutralinos is about 50%. In these models, N_1 is the LSP and assumed stable. The interpretation of the $ee\gamma\gamma$ which inspired our closer examination of this particular region of parameter space requires

$$\mathcal{B}(N_2 \to N_1\gamma) > 50\%. \tag{2.5}$$

In principle, one could look for this photon as an aid in selecting events with $t \to \tilde{t}N_2$. However, because of the large photino content of the N_2, its production in top decays is suppressed compared to N_1 or N_3. So rather than concentrate on a small fraction of events, we make no attempt to identify the photon in our study, and instead allow it to mimic a jet. Quite often, N_3 is also light enough to be produced by decaying tops. Its decays are more complicated: if the sneutrinos happen to be light enough to provide a 2-body channel, then $\tilde{\nu}\nu$ is favored; otherwise, the 3-body decays $N_1 f \bar{f}$ where f is a light fermion dominate. The net result is of all of this is that allowing the top to decay to SUSY states other than N_1 simply adds additional (relatively) soft jets to the final state.

B. The Supersymmetric Signal

Within the supersymmetric scenario proposed in Ref. [17], there are several different production mechanisms for top quarks, and hence many different final states which must be considered.

For the top pairs produced by the usual SM processes, we end up with mainly three different final states, depending upon the way in which they decay. Firstly, both tops could

decay to Wb, according to the Standard Model. In this case, the final state consists of 2 leptons, 2 jets, and missing p_T (dilepton); 1 lepton, 4 jets, and missing p_T (W + 4 jets); or 6 jets (all jets). Secondly, one top could decay to Wb, and the other to $\tilde{t}N_1$. In this case, the final state consists of 1 lepton, 2 jets, and missing p_T (W + 2 jets); or 4 jets and missing p_T (missing + 4 jets). Finally, both tops could decay to $\tilde{t}N_1$. In this case the final state consists entirely of 2 jets and missing p_T (missing + 2 jets). This last final state is identical to that of direct stop pair production, which is considerably more difficult because of the large Standard Model multijets background. Of the remaining final states coming from supersymmetric sources, the W + 2 jets mode is the most promising, and the one we will discuss in detail. In our illustrations, we will describe the situation where the top decays to a supersymmetric final state, and the antitop decays according to the Standard Model:

$$p\bar{p} \to t\bar{t} \to cN_1N_1\bar{b}\ell^+\bar{\nu}_\ell. \tag{2.6}$$

The presence of the charge-conjugated process is always implicitly assumed, and is included in all of the rates reported below.

In addition to (2.6), we must consider the effect of top quarks arising from gluino and squark decays, which, as argued in [17], must be present in significant numbers if the non-Wb top quark branching ratio is to be as large as is typical for a light stop. Top quarks produced in this manner are accompanied by extra jets. Consider first the pair production of gluinos. Both gluinos will decay to a top and a stop. The tops then decay as described above, and the stops each yield a charm jet and a neutralino. Thus, gluino pair production leads to the same final states as top pair production, but with two additional charm jets and additional missing energy. Likewise, for the chain beginning with a squark, we pick up an additional jet from the decay (2.1). For a summary of conventional gluino physics at FNAL, see Ref. [21].

It is useful to examine some kinematical consequences of the scenario we have proposed. Consider first purely SM $t\bar{t}$ production at the Tevatron, which takes place relatively close to threshold. We would expect the ordering in E_T of the $\bar{b}$ and c jets to reflect fairly accurately

the relative sizes of the t-W and $\tilde{t}$-N_1 mass splittings. For the range of masses we consider here, $m_t - m_W > \widetilde{M}_t - \widetilde{M}_{N_1}$. Hence, the highest E_T jet should come from the $\bar{b}$ quark most of the time. Our simulations confirm this, with the $\bar{b}$ quark becoming the leading jet more than 70% of the time over most of the range of SUSY masses examined. Fig. 2 shows the results for the kinematically allowed masses in the ranges 30 GeV $< \widetilde{M}_{N_1} <$ 70 GeV, 45 GeV $< \widetilde{M}_t <$ 100 GeV. The situation is only slightly worse when we add squark and gluino production. The additional jets from the cascade decays down to top are rather soft, given the relatively small mass splittings involved. Thus, in the all of the cases we examine here, the identification of the $\bar{b}$ parton with the leading jet is a reasonably good one.

Because the jets coming from gluino and squark decays are relatively soft, we will organize our results around the premise that the process (2.6) is the framework about which the complications from such decays are relatively small perturbations. That is, we will first describe the situation as if the only processes going on are the SM backgrounds plus decays of top to stop, parameterized by the stop mass, the LSP mass, and the branching ratio $\mathcal{B}(t \to \tilde{t}N_1)$ (Sec. IV). Then, we will expand our consideration to include a full-blown SUSY model where additional top quarks are being produced by decaying gluinos (Sec. V). As we shall see, the same superweight derived under the simplifying assumptions works well in the more realistic environment.

III. THE SUPERWEIGHT

We now describe a procedure which may be employed to construct a quantity we call the "superweight" out of the various observables associated with a given process. In principle, this procedure may be used to differentiate between signal and background in a wide range of processes, although we will concentrate on the detection of the decay (1.1).

For each event in the data sample passing our selection criteria (correct number and stiffness of jets, sufficient missing energy, correct number of leptons, *etc.*) we define a superweight $\widetilde{\mathcal{X}}$ by a sum of the form

$$\widetilde{\mathcal{X}} = \sum_{i=1}^{N} \mathcal{C}_i \tag{3.1}$$

where the $\mathcal{C}_i$'s evaluate to 0 or 1 depending upon whether or not some given criterion is satisfied. The number of terms N in the sum defining $\widetilde{\mathcal{X}}$ is arbitrary: one should use as many terms as there are "good" criteria. One could consider a more general form including separate weighting factors for the components and continuous values for the $\mathcal{C}_i$'s (as in a full-blown neural net analysis). However, our intent is to search for new particles over some range of masses and couplings. In such a situation, too much refinement could narrow the range of parameters to which the superweight is a good discriminant between signal and background. Furthermore, the components appearing in (3.1) are easily given a physical interpretation, which guides us in the optimization of the $\mathcal{C}$'s.

Let us consider a criterion of the form

$$\mathcal{C} = \begin{cases} 1, & \text{if } \mathcal{Q} > \mathcal{Q}_0; \\ 0, & \text{otherwise,} \end{cases} \tag{3.2}$$

where $\mathcal{Q}$ is some measurable quantity associated with the event, and $\mathcal{Q}_0$ is the cut point [22]. Although we will refer to $\mathcal{Q}_0$ as a cut point, we don't actually cut events from the sample which have $\mathcal{C} = 0$. Note that (3.2) implies that the value of $\mathcal{C}$ averaged over the entire sample is exactly the fraction of the cross section satisfying the constraint $\mathcal{Q} > \mathcal{Q}_0$. A "good" superweight component should have the property that its average for Standard Model events is much less than its average for SUSY events. That is, we want

$$\Delta\mathcal{C} \equiv \langle\mathcal{C}\rangle_{\rm SUSY} - \langle\mathcal{C}\rangle_{\rm SM} \tag{3.3}$$

to be as large as possible.

So, to develop a new superweight, one should first devise a set of cuts to produce a data set where the number of background events versus the number of signal events is reasonable (S:B of order 1:4, say). Next, separate Monte Carlos of both the signal and main backgrounds should be run, in order to generate plots of $\Delta\mathcal{C}$ as a function of $\mathcal{Q}_0$. The physical interpretation of $\langle\mathcal{C}\rangle$ as the fraction of events satisfying $\mathcal{Q} > \mathcal{Q}_0$ may be used

as a guide when deciding which $\mathcal{Q}_0$'s are worth investigating. For each value of the new physics parameters, there will be an ideal value of $\mathcal{Q}_0$ for which $|\Delta\mathcal{C}|$ is maximal. A good superweight component should not only have a "large" value of $|\Delta\mathcal{C}|$, but the corresponding value of $\mathcal{Q}_0$ at that point should be reasonably stable over the entire parameter space to be investigated.

An issue that arises concerns the question of correlations among the $\mathcal{C}_i$'s. Our philosophy in this respect is to evaluate the effectiveness of the superweight in terms of how well it separates the signal from the background, *i.e.* what is the purity of an event sample with a certain minimum superweight? Thus, while we avoid using two $\mathcal{C}_i$'s whose values are 100% correlated (on the grounds that doing so is no more beneficial than using only one of the two), we don't worry about using partially correlated $\mathcal{C}_i$'s. The main effect of correlations among the $\mathcal{C}_i$'s is that the overall performance of the sum of the $\mathcal{C}_i$'s will be less than what is implied by considering the $\mathcal{C}_i$'s individually. Thus, to evaluate the effectiveness of a given superweight definition, one should compare the predicted distributions in $\widetilde{\mathcal{X}}$ for the signal and background.

We now give an example of the steps used to determine one of the superweight elements for the $t \to \tilde{t}N_1$ search method described in detail in Sec. IV. To begin, we take a moment to recall the definition of the transverse mass. Given particles of momenta P and Q, the transverse mass of the pair is defined by

$$m_T^2(P,Q) = 2P_T Q_T[1 - \cos\Phi_{PQ}], \tag{3.4}$$

where $P_T \equiv \sqrt{P_x^2 + P_y^2}$ and Φ_{PQ} is the azimuthal opening angle between P and Q. An important feature of the transverse mass is that if the particles P and Q were produced in the decay of some parent particle X, then the maximum value of $m_T(P,Q)$ is precisely the mass of X.

As already discussed in Sec. II, the signal (2.6) for top to stop appears in the detector as a charged lepton, 2 jets, and missing energy. The largest background turns out to be the Standard Model production of a W plus 2 jets, so we determine our superweight criteria

using that background. Furthermore, we know that for signal events, the leading jet is usually from the $\bar{b}$ quark in the $\bar{t} \to W^- \bar{b}$ decay. Consequently, most of the time the leading jet and the charged lepton should reconstruct to no more than the top quark mass (some energy and momentum is carried away by the unseen neutrino). This suggests an upper limit on the value of $m_T(j_1, \ell)$, which may violated at least some of the time by ordinary W plus 2 jet events. In Fig. 3, we show the differential cross section in $m_T(j_1, \ell)$ for both the signal and the background, as determined from VECBOS [23] (relevant details of our simulations will be discussed in Sec. IV). Note that for the signal there is the expected sharp drop-off for large values of $m_T(j_1, \ell)$. In Fig. 4 we show the fraction of events with a $j_1\ell$ transverse mass above $m_T(j_1, \ell)$, as a function of $m_T(j_1, \ell)$. The individual magnitudes of these two curves are not critical in making a good superweight component, but rather the difference in these two curves, which is plotted in Fig. 5 not only for the masses used in Figs. 3 and 4, but also for two additional values as well. The presence of a dip ranging in depth from about -0.4 to -0.5 in the vicinity of $m_T(j_1, \ell) = 125$ GeV for each of the masses used suggests that this is indeed a worthwhile superweight element, and that the criterion should read

$$\mathcal{C} = \begin{cases} 1, & \text{if } m_T(j_1, \ell) < 125 \text{ GeV}; \\ 0, & \text{otherwise.} \end{cases} \tag{3.5}$$

The key quantities to look for in this evaluation were approximate stability in peak (dip) position and "large" magnitude for the peak for the range of parameters to be investigated. Narrowness of the peak is not a requirement. In fact, a broad peak is better, since then the exact placement of the cut point is unimportant. Note also that since we are exploiting the difference in the *shapes* of the signal and background distributions, there is no reason we can't use an observable both for cutting and in the superweight. For example, even after requiring a minimum missing transverse momentum, we can (and do) still use a superweight criterion based on the shapes of the missing transverse momentum distributions for the surviving events.

IV. THE PROCESS $p\bar{p} \to t\bar{t} \to cN_1N_1\bar{b}\ell^+\bar{\nu}_\ell$

Our simulations of the signal and backgrounds in this section are based upon tree level matrix elements, with the hard-scattering scale for the structure functions and first-order running α_s set to the partonic center of mass energy. For vector-boson plus jet production, we employ VECBOS [23] running with the structure functions of Martin, *et. al.* [24] (the "BCDMS fit"). For the processes containing top pairs, we perform a Monte Carlo integration of the matrix element folded with the HMRS(B) structure functions [25]. Under these conditions, the tree-level SM $t\bar{t}$ production cross section is 5.1 pb for 163 GeV top quarks, while two recent computations of the NLO rate including the effects of multiple soft gluon emission give $6.95^{+1.07}_{-0.91}$ pb [26] and $8.12^{+0.12}_{-0.66}$ pb [27] for this mass, implying a K factor in the 1.4 to 1.6 range. We refrain from applying any K factor to the rates we report below, although the reader may wish to do so. On the the other hand, we do use a somewhat light value of m_t (163 GeV).

Hadronization and detector effects are mocked up by applying gaussian smearing with a width of $125\%/\sqrt{E} \oplus 2.5\%$. When the simulation of merging jets is called for, we combine final state partons which lie within 0.4 units of each other in (η, ϕ) space. Since our intent is to demonstrate that the superweight method is viable, we have avoided detailed simulation of the CDF or D0 detectors. Instead, we have tried to capture enough of the general features in order to demonstrate the viability of the method. Of course, the superweight criteria used in an actual analysis should be determined by the experimenters from a complete detector simulation.

A. Discussion of Backgrounds

There are several ways to mimic our signal of a hard lepton, missing E_T, and two (or more) jets within the Standard Model. The most obvious background process, and the one with the largest raw cross section is the direct production of a W plus 2 jets. However, we

can also have contributions from Z plus 2 jets should one of the leptons be missed by the detector. Furthermore, we must beware of Standard Model sources of top quarks. In the context of $t\bar{t}$ production, the dilepton mode can fake the signal if one of the two leptons is lost, which is particularly likely if one of the W's decays to $\tau\nu$. Since τ leptons, can appear as either a jet of hadrons plus missing momentum ($\tau \to j\nu_\tau$) or as a lepton plus missing momentum ($\tau \to \ell\bar{\nu}_\ell\nu_\tau$), we have been careful to study these backgrounds separately. The $W + 4$ jets mode is also a potential troublespot, since jets can merge or simply be too soft to be detected. Finally, single top production followed by SM top decay leads to a final state of a W, two b jets, and missing energy (plus possibly an extra jet if W-gluon fusion is the production mechanism). Fortunately, the small rate for single tops is effectively dealt with by the cuts described below.

The cuts we impose on the data before embarking on our superweight analysis are listed in Table I. The entries above the dividing line are our "basic" cuts. They were inspired by the CDF top analysis [28], in order to automatically incorporate some of the coverage and sensitivity limitations imposed by the detector, and to produce a "clean" sample of events. Thus we require the lepton to have a minimum p_T of 20 GeV, be centrally located ($|\eta| < 1$) and to lie at least 0.4 units in ΔR from the jets ($\Delta R \equiv \sqrt{(\Delta\eta)^2 + (\Delta\varphi)^2}$). The p_T cut on the lepton aids in the rejection of taus which decay leptonically. Some discrimination against events with fake missing E_T is obtained by setting a minimum $\not\!\!E_T$ of 20 GeV. The leading two jets should each have a p_T of at least 15 GeV, and a pseudorapidity $|\eta| < 2$. All jets must have a minimum separation of 0.4 units in ΔR.

To reject Standard Model $t\bar{t} \to W + 4$ jets events, we require that the third hardest jet have a *maximum* p_T of 10 GeV. While effective in this task, such a cut does have the unwanted side-effect of suppressing signal events containing extra jets, such as those containing squarks and gluinos [17]. In addition, some signal events will contain extra jets because of QCD radiation. Inclusion of either class of events in the data sample requires the relaxation of this cut, as is done in Sec. V. Here we note that the data in Table VIII imply that no more than 25% of the signal events contain extra jets above 10 GeV in p_T,

so the ultra-conservative reader may wish to reduce the signals we report in this section by that amount. However, since we have neglected a K factor of 1.4–1.6 in our figures, we feel that our values are indeed reasonable.

Table II lists the sources of background discussed above along with the estimated cross section surviving the cuts for each mode. Note that we report the $t\bar{t}$ backgrounds as if $\mathcal{B}(t \to Wb)$ were unity: the actual contributions to the background in the presence of a signal are smaller by a factor of this branching ratio squared. While the basic cuts are nearly adequate for most of the backgrounds, the contribution from $W + 2$ jets is still an overwhelming 39.1 pb, necessitating an additional cut. Given an ideal detector, the only source of missing momentum in a background $W + 2$ jet event is the neutrino from the decaying W. Hence, the transverse mass of the charged lepton and missing momentum (energy) must be less than or equal to the W mass. Allowing for the finite width of the W as well as detector resolution effects, a number of events spill over into higher m_T values. In contrast, for SUSY events given by (2.6), the presence of the two neutralinos in addition to the neutrino frequently produces events with a transverse mass well above m_W. Thus, we require that $m_T(\ell,\, \not{p}_T) > 100$ GeV. This cut is highly effective against the $W + 2$ jets background, while preserving about half of the remaining signal. It also removes the small contribution from single top production. However, it is less effective against the $t\bar{t}$ backgrounds, especially those containing τ's. Fortunately, those backgrounds are already under control.

When all of our cuts are imposed, the surviving background is about 0.42 pb, nearly 90% of which comes from Standard Model production of a W plus 2 jets. Hence, we consider only that background in developing the $\mathcal{C}$'s that make up the superweight.

We plot the efficiency for retaining the signal in Fig. 6 as a function of the stop and LSP masses, and supply numerical values for several representative pairings in Table III.

B. Construction of the Superweight

In Table IV we list the 10 criteria used to build the superweight for the process (2.6), in approximate order of decreasing usefulness. We now provide intuitive explanations for our selections: although the exact placement of the cut points is determined from the Monte Carlo, we should still be able to understand from a physical point of view why criteria of the forms listed are sensible.

We begin our discussion with the three criteria ($\mathcal{C}_5$, $\mathcal{C}_8$, and $\mathcal{C}_9$) which depend on joint properties of the charged lepton (ℓ) and leading jet (j_1). As already discussed in Sec. II, the $\bar{b}$ quark frequently becomes the leading jet. Since the $\bar{b}$ quark and the charged lepton come from the same parent top quark, not only would we expect an upper limit on the mass of the pair ($\mathcal{C}_9$, discussed previously), but there should be some tendency for the lepton and jet 1 to align. On the other hand, in Standard Model W + 2 jet events, the W is recoiling against the two jets, leading to a tendency for the lepton and jet 1 to *anti*-align. Hence, we adopt $\mathcal{C}_5$, which contributes when the j_1-ℓ azimuthal angle is less than 2.4 radians, and $\mathcal{C}_8$, which contributes when the cosine of the j_1-ℓ opening angle is greater than -0.15.

The next group of criteria ($\mathcal{C}_1$, $\mathcal{C}_2$, $\mathcal{C}_6$, $\mathcal{C}_7$) are various combinations of the transverse momenta in the event. Naturally, we make use of the "classic" supersymmetric signature: the missing transverse momentum ($\mathcal{C}_1$), which we require to be at least 65 GeV to add one unit to the superweight, that being the point where the two integrated fractions differ the most. In addition, we make use of the fact that Standard Model W + 2 jets production falls off rapidly with increasing p_T; that is, we expect the lepton and jets from the signal process to be somewhat harder on average. Instead of the individual p_T's, however, we use their scalar sum with the missing p_T. Admittedly, there are some correlations introduced by this choice; however, as discussed in Sec. III, that is not important for our purposes.

The remaining criteria ($\mathcal{C}_3$, $\mathcal{C}_4$ and $\mathcal{C}_{10}$) may be described as "miscellaneous." The first of these is tied to the difference between the missing p_T and charged lepton p_T,

$$\Delta\mathcal{P}_T \equiv p_T(miss) - p_T(\ell). \tag{4.1}$$

In Standard Model events, the neutrino from the decaying W-boson is the only source of missing momentum. Even though the 2-body decay of a polarized W-boson is not isotropic in its rest frame, we expect little or no net polarization in the W bosons produced at the Tevatron. Consequently, the distribution in $\Delta\mathcal{P}_T$ ought to be symmetric about zero: there is no preferred direction for the charged lepton relative to the W boost direction. On the other hand, for events with a supersymmetric origin, there are a pair of N_1's in the final state. On average, these neutralinos will tend to increase the mean value of the missing transverse momentum. Hence, we expect that the distribution in $\Delta\mathcal{P}_T$ will be asymmetric, with a peak for some positive value. We find that a criterion reading $\Delta\mathcal{P}_T > 0$ GeV is useful.

Earlier, we commented on the use of the transverse mass of the charged lepton and missing p_T for the purpose of reducing the W + 2 jets background. Among the events satisfying this cut, the distributions *still* differ enough to produce a useful superweight criterion: the spectrum of Standard Model events falls more rapidly than for the SUSY events. Thus, we select a criterion of the form $m_T(\ell,\, \not{p}_T) > 125$ GeV ($\mathcal{C}_4$).

The final criterion we employ is the "visible" mass, defined by summing the observed 4-momenta of the charged lepton and the leading two jets, and forming an invariant mass-squared. If all of the final state particles were represented by these three objects, then this quantity would be equal to the center of mass energy squared of the hard scattering, that is $\gtrsim 2m_t$ for the signal, and $\gtrsim 2M_W$ for the background. However, not all of the particles are detected: some go down the beampipe, some are too soft, and some are weakly interacting. We expect the first two kinds of losses to be comparable across signal and background. In contrast, since the signal events contain two extra weakly-interacting particles (the N_1's), an even larger proportion of the total mass is invisible. Although it is not immediately obvious which way the net effect will go, it is clear that that distributions in this variable should be different. From a study like the one described in Sec. III, we find that we should set $\mathcal{C}_{10} = 1$ when $m(\ell, j_1, j_2) < 200$ GeV.

C. Results

The procedure we have in mind for the detection of top to stop decays is a simple counting experiment. We apply all of the cuts in Table I to the data, and evaluate the superweight for each of the surviving events. Our signal consists of an excess of events which have a superweight greater than some value determined by comparing the expected superweight distributions for the signal and background.

We now consider various pieces of data relevant to evaluating the effectiveness of the superweight we have just defined. Fig. 7 shows the distribution of signal events according to their superweight, for the specific masses $\widetilde{M}_t = 65$ GeV, $\widetilde{M}_{N_1} = 45$ GeV. A significant tendency for signal events to have a high superweight is readily apparent. Fig. 8 presents the mean value of $\widetilde{\mathcal{X}}$ as a function of the stop and neutralino masses for kinematically allowed points in the range $45 \text{ GeV} \leq \widetilde{M}_t \leq 100 \text{ GeV}, 30 \text{ GeV} \leq \widetilde{M}_{N_1} \leq 70 \text{ GeV}$. Note the flatness of this distribution: this implies that our superweight has roughly the same effectiveness over the entire range. Numerical results are presented in Table V for a few selected points. Over the entire range the mean superweight is in excess of 7, and typically 75% or more of the events have a superweight of 6 or greater.

Of course, the significance of these results depends upon the behavior of the backgrounds. We plot the superweight distributions for all backgrounds which were estimated to be 1 fb or greater in Fig. 9, and supply the mean values and fraction of events of each type with superweights of 6 or greater in Table VI. It is readily apparent that our criteria were tailored to reject W + 2 jets events: they do that very well. On the other hand, the backgrounds from Standard Model $t\bar{t}$ production do not typically have low superweights. In fact, their superweight distributions resemble that of the signal. Fortunately, the cross section times branching ratio surviving our cuts for such events is only 0.023 pb (0.006 pb if we include the effect of $\mathcal{B}(t \to \tilde{t}N_1) = 50\%$), while for most (but not all) values of the SUSY masses, the signal has a cross section 3 to 5 times greater than this particular background.

To get a feeling for the range of masses to which we are sensitive, we present Fig. 10,

which shows the predicted number of signal events in 100 pb^{-1} of data, the approximate size of the present CDF and D0 data sets. To guide the eye, we have included the contour where $S/\sqrt{B} = 3$. We must caution the reader, however, that the exact area in which we can exclude or discover the top squark depends upon a more complete analysis involving full detector simulations and Poisson statistics where appropriate. Note that the numbers in Fig. 10 assume a 50% branching ratio of top to stop (which is the most favorable case). However, we have omitted the expected increase in rate from the 1–loop radiative corrections and summation of multiple soft gluon emission. Furthermore, we have reported $t\bar{t}$ backgrounds that do not include the effects of the reduced branching ratio to Wb. So overall, we believe our numbers to be reasonably conservative. One might hope to increase the signal somewhat by a careful tuning of the cut choices in Table I and the superweight definition in Table IV. Also, in the event that a signal is found, it would be useful to vary the final cut on the superweight, as a check on systematics.

It is interesting to compare our results to those of Mrenna and Yuan [16], who consider the same search, but only employ cuts on the "traditional" event observables. They obtain a background of 1.8 events for 100 pb^{-1} of data [29], compared to our 4.9 events in the $\widetilde{\mathcal{X}} \geq 6$ sample. However, the efficiencies they report for retaining the signal are only in the 6%–8% range: our efficiencies are as high as 16%. The net result is that we have a larger $S/\sqrt{B}$: indeed, their $S/\sqrt{B} = 3$ contour would lie somewhere in the vicinity of the $N = 8$ contour on our Fig. 10.

Conspicuously absent from our discussion to this point has been the issue of b-tagging. We have avoided using such information so far for two reasons. First, the efficiency for b-tagging reported by CDF is currently about 30% per b jet [30]. Hence, the rejection of events without a b-tag lowers the efficiency significantly. Furthermore, this tagging efficiency implies that a superweight criterion reading

$$\mathcal{C} = \begin{cases} 1, & \text{if there is a } b\text{-tag} \\ 0, & \text{otherwise,} \end{cases} \tag{4.2}$$

only adds about 0.3 units of separation in the mean superweights of the signal and back-

ground. Compared to the criteria already in use, this is only a modest separation. Therefore, we would prefer to use b-tagging to verify that the high superweight events do indeed contain top quarks in the event that a signal is observed. Note that this assessment would change should the tagging algorithms improve: we urge the experimentalists to vary the parameters and criteria in Tables I and IV to obtain the optimum balance. Finally, given that the SUSY signal contains both a b jet and a c jet, we remark that the development of a specific charm-tagging algorithm would be useful in this connection.

V. INCLUSION OF SQUARKS AND GLUINOS

In this section we consider our superweight analysis in the context of a "complete" SUSY model. Our aim is to demonstrate that the addition of other sources of top quarks can only help in the observability of a signal, if present. At the same time, we will show that it is indeed sufficient to tune the superweight criteria using the simplified assumptions of Sec. IV. To illustrate these points, we have chosen a specific model which has a stop mass of 65 GeV and a LSP mass of 45 GeV: we believe this model to be representative of the types of models described in Sec. II. We list a few other features of this model in Table VII.

The data in this section were generated using `PYTHIA 5.7` [31] with supersymmetric extensions [32]. Tree level matrix elements are used, along with the CTEQ2L structure functions [33]. The square of the hard-scattering scale for the structure functions and first-order running α_s is set to the average of the squares of the transverse masses of the two outgoing particles participating in the hard scattering (the program default). For this choice of calculational parameters, the raw SM $t\bar{t}$ production cross section is reported as 6.8 pb, which is rather close to the NLO estimates. Although we do not do so, the reader may wish to apply a K factor of 1.0–1.2 to the signals we report in this section.

Jets are constructed using a cone algorithm ($R = 0.7$) inside a toy calorimeter using the routine supplied by `PYTHIA`. No attempt is made to simulate the out-of-cone corrections required to ensure that the jet energy accurately reflects the parton energy. Thus the output

systematically underestimates the jet energies. As a result, it is not possible to directly compare the results appearing in this section with the results from the previous section. In particular, the efficiencies implied by the data in this section will be lower than what should be expected under actual conditions. This merely underscores the importance of having each experiment do the analysis with their full detector simulations in place. Our goal in this section is to document the effect of adding SUSY-induced $t\bar{t}$ production mechanisms to the analysis, and so the only direct comparisons we need to make to this end are self-contained within this set of Monte Carlos.

In order to take advantage of the SUSY-produced top events, we must relax our cut on the p_T of the third jet. However, we must beware of the background represented by W + 4 jet SM decays of the top. In Fig. 11 we compare the p_T distributions of the third jet for signal ($\tilde{g}\tilde{g}$, $\tilde{q}\tilde{q}$, and $\tilde{g}\tilde{q}$) and $t\bar{t} \rightarrow W + 4$ jets background, employing the cuts in Table I *except* for the requirement on the third jet. It is apparent from Fig. 11 that it is possible to raise the cut on the maximum allowed p_T of the third jet without totally swamping the signal in SM $t\bar{t}$ background. We will present our results for the cases $p_T(j_3) < 10, 20, 30$ GeV.

Table VIII lists the number of events in 100 pb^{-1} predicted to pass the cuts in Table I, as a function of the maximum allowed p_T of jet 3. The entries above the dividing line are within the context of our SUSY model. For the purposes of this study, we define as "signal" any event which contains a pair of N_1's in the final state, whether or not it contains a $t \rightarrow \tilde{t}c$ decay. Thus, we list separate entries for $t\bar{t}$ events which contain at least one SUSY decay ($t\bar{t}$ signal) and those which don't ($t\bar{t}$ background), but do not distinguish between squark and gluino events which do or do not contain tops in the intermediate states. Should a SUSY scenario of this type prove to be correct and one wanted to study only $t \rightarrow \tilde{t}c$ events, additional work would be required to purify the sample to remove these non-$t\bar{t}$ SUSY "backgrounds." Note that, as expected, for the tightest $p_T(j_3)$ cut (10 GeV), the squark and gluino channels have little effect on the expected number of events. However, by relaxing this cut to 30 GeV, we allow nearly 2/3 of the $\tilde{g}\tilde{g}$, $\tilde{q}\tilde{q}$, and $\tilde{g}\tilde{q}$ events into the sample, with only a modest increase in the background from SM $t\bar{t}$ decays.

The entries below the line give the number of counts assuming purely SM $t\bar{t}$ production and decay. For good discriminating power, the cuts on j_3 and the superweight should be chosen so that the total number of counts expected with SUSY is greatly different from the total number of counts expected without SUSY. Since the background from W/Z + jets in the absence of a superweight cut (nearly 40 events) is significantly larger than the entries in Table VIII, it is necessary to impose such a cut. Fig. 12 shows the superweight distribution for the signal (N_1-containing) events. Compared to Fig. 7, we see a somewhat broader distribution. However, there is still a significant peaking at high superweight, and the cut $\widetilde{\mathcal{X}} \geq 6$ still retains the majority of the signal (73% in this case). Hence, we present Table IX, which is the same as Table VIII, but with the additional requirement $\widetilde{\mathcal{X}} \geq 6$. Now the W/Z + jets background is reduced to the point where, for example, taking the $p_T(j_3)$ cut to be at 30 GeV yields a factor of 2 difference in the number of counts with and without SUSY. Thus, the prospects for observing or excluding this type of model are quite good.

VI. CONCLUSIONS

We have investigated the possibility of detecting a light stop squark in the decays of top quarks using the present Fermilab Tevatron data set (approximately 100 pb^{-1}). Instead of a traditional analysis which relies on cutting on the kinematic observables individually with a low resultant efficiency, we have defined a composite observable, the superweight. The superweight is assigned event-by-event depending upon how many of the criteria from a predetermined list are true. By construction, events with a large superweight are likely to be signal, while those with a small superweight are likely to be background. Since we do not require *all* of the criterion to be true to accept an event, our efficiency is significantly better; for example, compared to the analysis of Mrenna and Yuan [16], our signal efficiencies are typically twice as large. For the given set of cuts and superweight criteria, we have shown that the prospects for finding a top-to-stop signal are good. Fig. 10 can be viewed as a summary of the results. The collaborations are urged to view this work as a starting point,

since a proper analysis must be based upon the actual event reconstruction program used by each experiment. Furthermore, by adjusting the parameters in Tables I and IV it may be possible to do even better.

Finally, we remark that although we have applied the superweight concept to the specific case of a light stop squark in supersymmetric models, the method is applicable in any situation where the individual kinematic cuts required to reduce the background result in a low signal efficiency. Thus, for example, one could consider developing a superweight suited for the direct search for stop pair production.

ACKNOWLEDGMENTS

High energy physics research at the University of Michigan is supported in part by the U.S. Department of Energy, under contract DE-FG02-95ER40899.

GDM would like to thank Soo–Bong Kim, Graham Kribs, Steve Martin, Steve Mrenna, and Stephen Parke for useful discussions.

REFERENCES

* Electronic address: mahlon@umich.edu

† Electronic address: gkane@umich.edu

[1] S. Park, "Search for New Phenomena in CDF," 10th Topical Workshop on Proton-Antiproton Collider Physics, edited by Rajendran Raja and John Yoh, AIP Press, 1996.

[2] See the Rapporteur talks of A. Blondel, S. Polorski, and A. Buras at the XXVIII International Conference on High Energy Physics, Warsaw, July 1996.

[3] M. Shifman, Mod. Phys. Lett. **A10**, 605 (1995).

[4] J.D. Wells and G.L. Kane, Phys. Rev. Lett. **76**, 869 (1996).

[5] J.D. Wells, C. Kolda, and G.L. Kane, Phys. Lett. **B338**, 219 (1994).

[6] G.L. Kane and J.D. Wells, Phys. Rev. Lett. **76**, 4458 (1996).

[7] J. Erler and P. Langacker, Phys. Rev. **D52**, 441 (1995); G.L. Kane, R. Stuart, and J.D. Wells, Phys. Lett. **B354**, 350 (1995).

[8] S. Ambrosanio, G.L. Kane, G.D. Kribs, Stephen P. Martin, and S. Mrenna, Phys. Rev. Lett. **76**, 3498 (1996).

[9] S. Dimopolous, M. Dine, S. Raby, S. Thomas, Phys. Rev. Lett. **76**, 3494 (1996).

[10] H. Baer, M. Drees, R. Godbole, J. Gunion, and X. Tata, Phys. Rev. **D44**, 725 (1991).

[11] H. Baer, J. Sender, and X. Tata, Phys. Rev. **D50**, 4517 (1994).

[12] J.L. Lopez, D.V. Nanopoulos, and A. Zichichi, Mod. Phys. Lett. **A10**, 2289 (1995).

[13] K.J. Abraham, F. Cuypers, and G.J. van Oldenborgh, Report No. hep-ph/9501401, 1995 (unpublished).

[14] J. Sender, Phys. Rev. **D54**, 3271 (1996).

[15] K. Hikasa and M. Kobayashi, Phys. Rev. **D36**, 724 (1987).

[16] S. Mrenna and C.P. Yuan, Phys. Lett. **B367**, 188 (1996).

[17] G.L. Kane and S. Mrenna, Report No. hep-ph/9605351, 1996 (to appear in Phys. Rev. Lett.).

[18] T. Kon and T. Nonaka, Phys. Rev. **D50**, 6005 (1994).

[19] S. Abachi, *et. al.*, Phys. Rev. Lett. **76**, 2222 (1996).

[20] P. Mättig, talk at the XXVIII International Conference on High Energy Physics, Warsaw, July 1996.

[21] H. Haber, "Phenomenology of Gluino Searches at the Tevatron," in *Supersymmetry and Unification of Fundamental Interaction (SUSY 93)*, Boston, MA, 1993, edited by P. Nath, (World Scientific, Singapore, 1993), p. 373.

[22] We are, of course, free to require instead $\mathcal{Q} < \mathcal{Q}_0$ for a non-zero contribution to the superweight. Our discussion applies to this case as well, with obvious modifications.

[23] F.A. Berends, H. Kuijf, B. Tausk, and W.T. Giele, Nucl. Phys. **B357**, 32 (1991); W.T. Giele, E. Glover, D. Kosower, Nucl. Phys. **B403**, 633 (1993).

[24] A.D. Martin, R.G. Roberts, W.J. Stirling, Phys. Lett. **206B**, 327 (1988).

[25] P. Harriman, A. Martin, R. Roberts, and W.J. Stirling, Phys. Rev. **D42**, 798 (1990).

[26] S. Catani, M.L. Mangano, P. Nason, L. Trentadue, Phys. Rev. Lett. **B378**, 329 (1996). The value we quote is based upon the fit (valid over the range 160 GeV $< m_t <$ 190 GeV) these authors give for their result,

[27] E. Berger, H. Contopanagos, Phys. Rev. **D54**, 3085 (1996). The value we quote is taken from interpolation of the values reported in Table I.

[28] F. Abe, *et. al.*, Phys. Rev. Lett. **74**, 2626 (1995).

[29] The authors of Ref. [16] *include* the effects of the reduced $t \to Wb$ branching ratio when computing the total background rate. If these effects are ignored, their background increases to 4.3 events, implying that $S/\sqrt{B} < 3$ for all of the mass pairs they investigate.

[30] D. Amidei and R. Brock, eds., "Future Electroweak Physics at the Fermilab Tevatron," Fermilab Report No. FERMILAB–PUB–96/046, 1996 (unpublished).

[31] H.U. Bengtsson and T. Sjöstrand, Comp. Phys. Comm. **46**, 43 (1987).

[32] S. Mrenna, "Simulating Supersymmetry with `PYTHIA 5.7` and `JETSET 7.4`," CITHE–68–1987, July 1995.

[33] J. Botts, *et. al.*, Phys. Lett. **B304**, 159 (1993); Michigan State University Report No. MSUHEP 93-18, 1993 (unpublished).

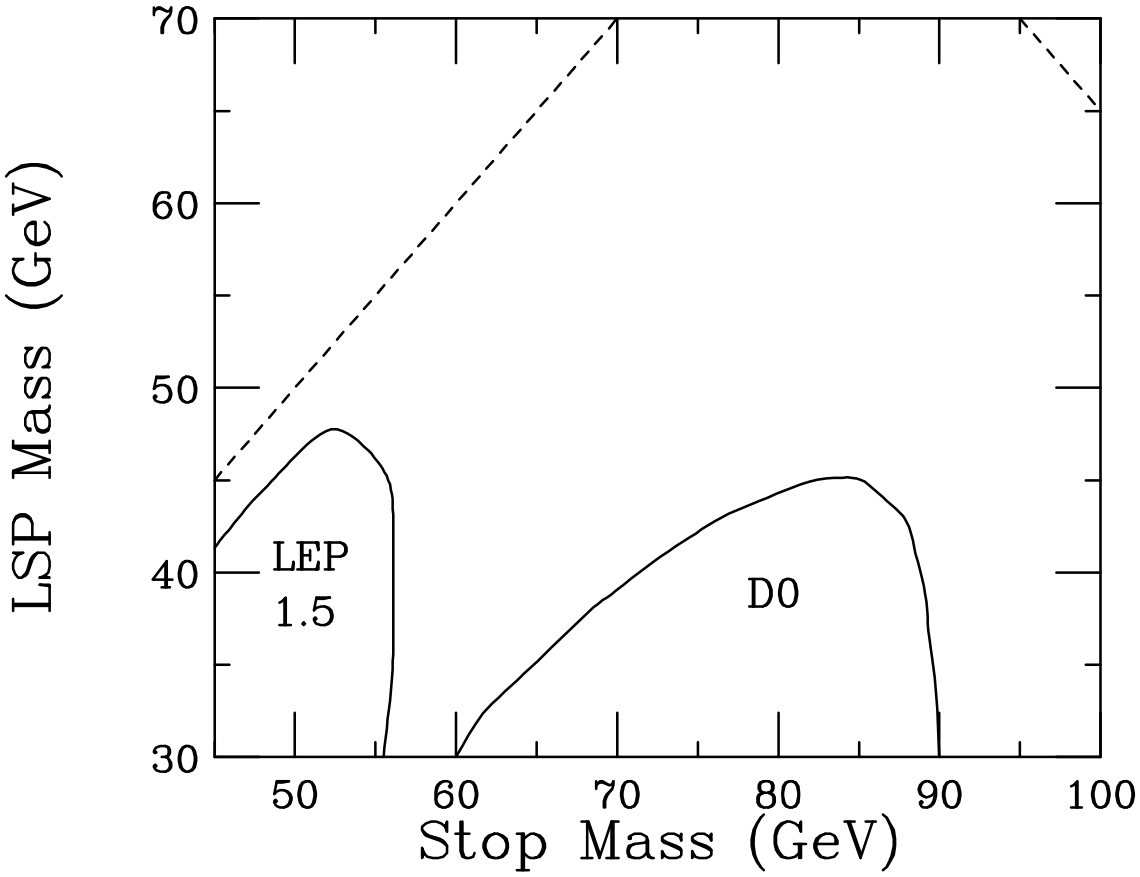

FIG. 1. Regions of the $\widetilde{M}_t$-$\widetilde{M}_{N_1}$ mass plane excluded by D0 [19] and LEP 1.5 [20]. The area above the dashed line is kinematically forbidden.

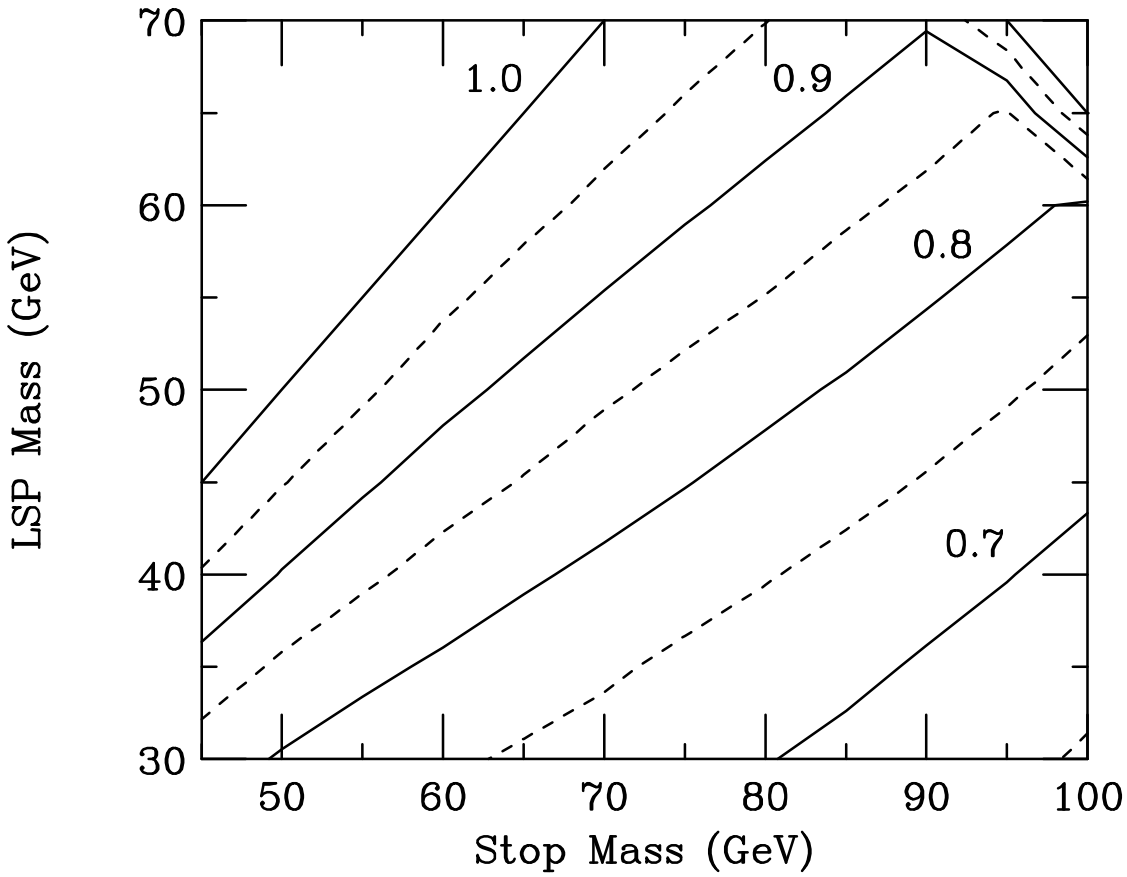

FIG. 2. Fraction of $t\bar{t} \to cN_1N_1\bar{b}\ell^+\bar{\nu}_\ell$ events surviving all of the cuts in Table I for which the $\bar{b}$ quark becomes the highest E_T jet (j_1), as a function of the stop and LSP masses. The contour labeled 1.0 is also the kinematic limit.

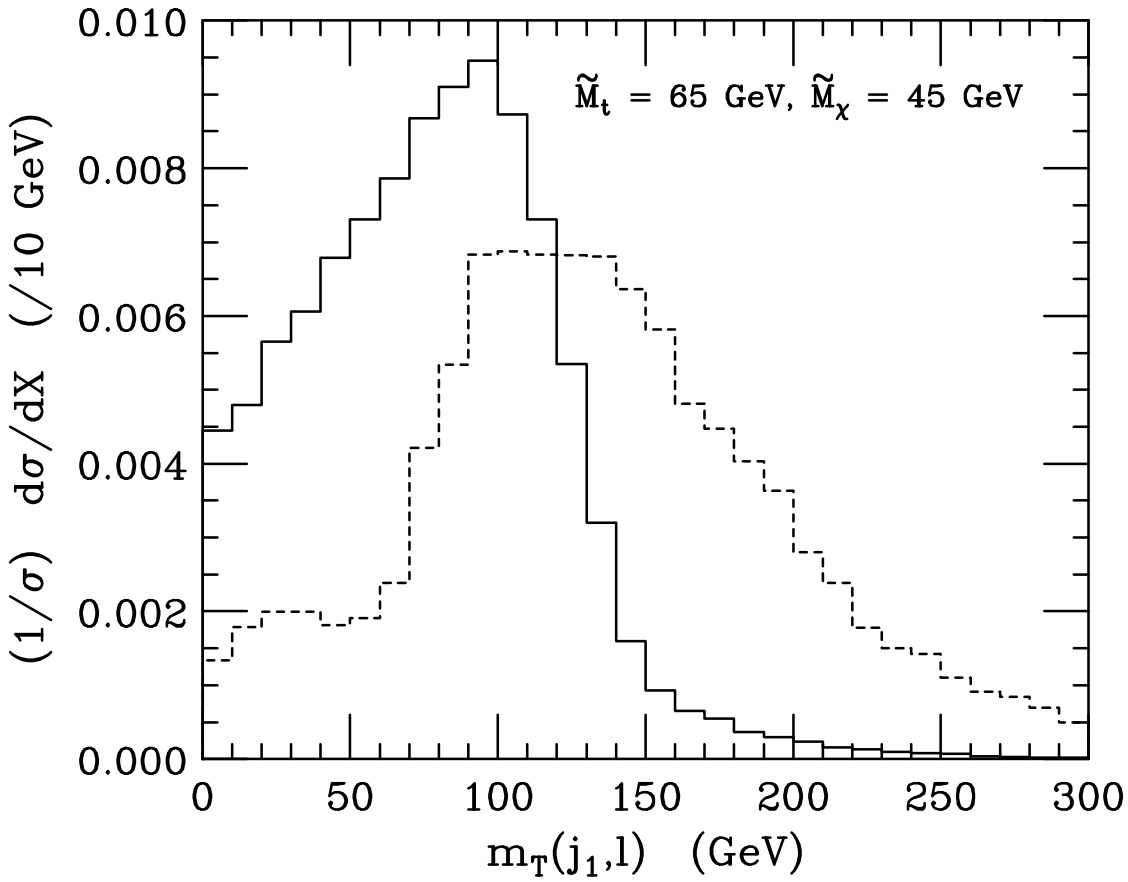

FIG. 3. Differential distribution of the $j_1\ell$ transverse pair mass for Standard Model $W + 2$ jets production (dashed) and $t\bar{t} \to cN_1N_1\bar{b}\ell^+\bar{\nu}_\ell$ (solid). We take $\widetilde{M}_t = 65$ GeV and $\widetilde{M}_{N_1} = 45$ GeV. Only events passing all of the cuts in Table I are included. Both histograms have been normalized to unit area.

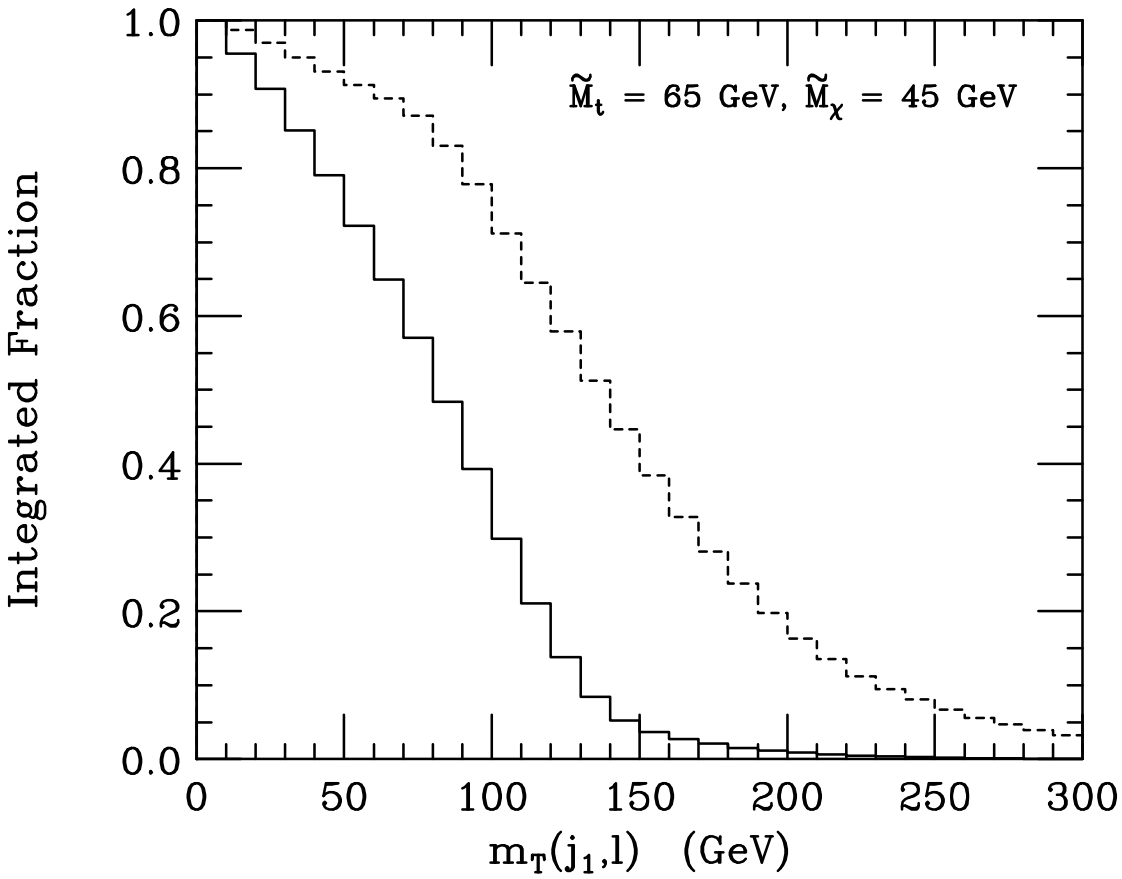

FIG. 4. Fraction of events with a $j_1\ell$ transverse pair mass above $m_T(j_1,\ell)$ for Standard Model W + 2 jets production (dashed) and $t\bar{t} \to cN_1N_1\bar{b}\ell^+\bar{\nu}_\ell$ (solid). We take $\widetilde{M}_t = 65$ GeV and $\widetilde{M}_{N_1} = 45$ GeV. Only events passing all of the cuts in Table I are included.

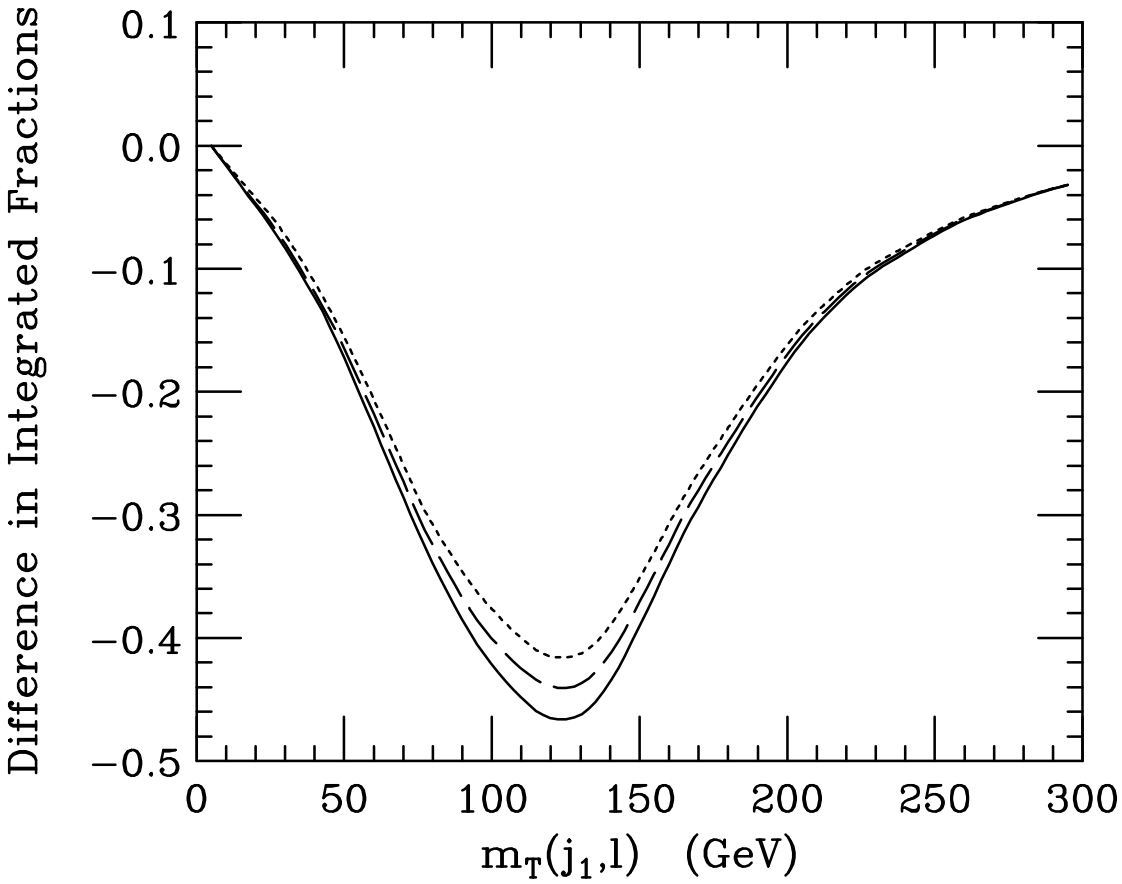

FIG. 5. Difference in integrated fractions, as defined by equation (3.3), for the observable $m_T(j_1, \ell)$. The mass values $(\widetilde{M}_t, \widetilde{M}_{N_1})$ in GeV for each line are: $(50, 40)$ solid, $(65, 45)$ dashed, $(85, 50)$ dotted.

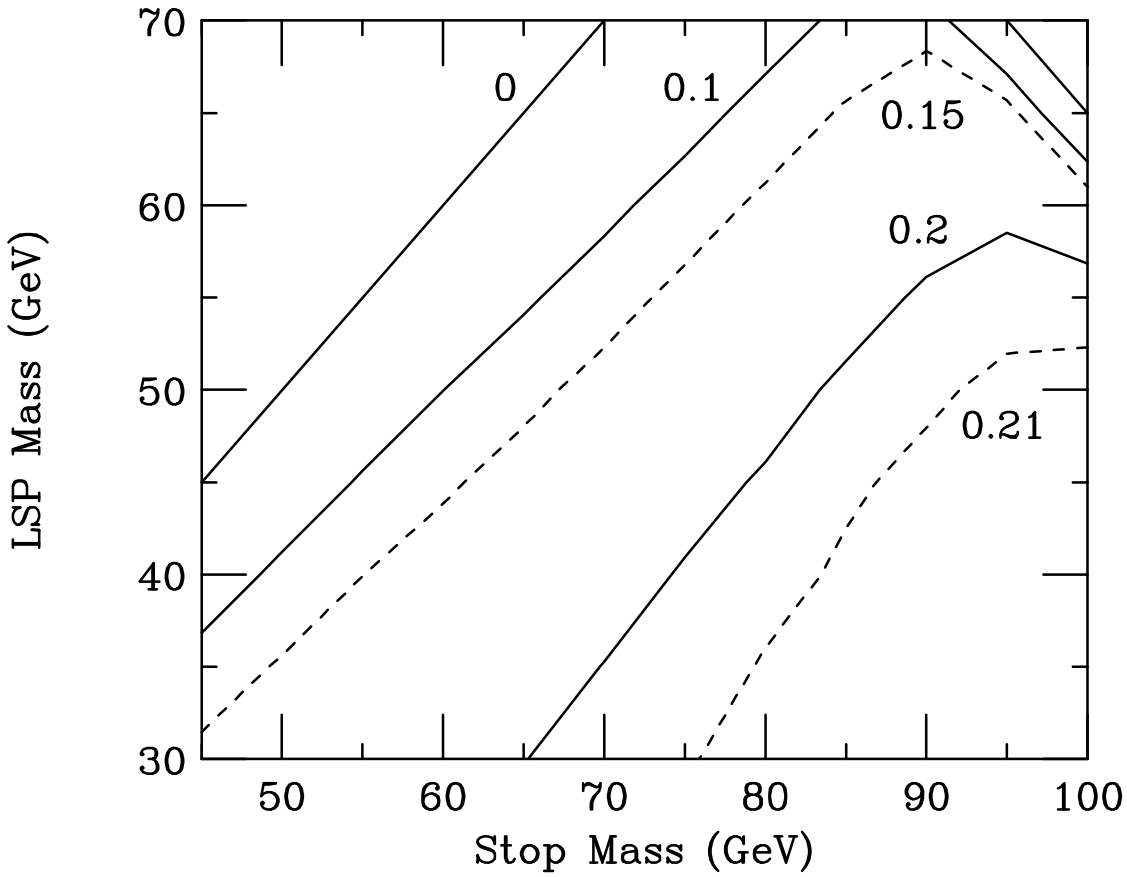

FIG. 6. Fraction of $t\bar{t} \to cN_1N_1\bar{b}\ell^+\bar{\nu}_\ell$ events surviving all of the cuts in Table I, as a function of the stop and LSP masses. The efficiency drops to zero at the kinematic limit.

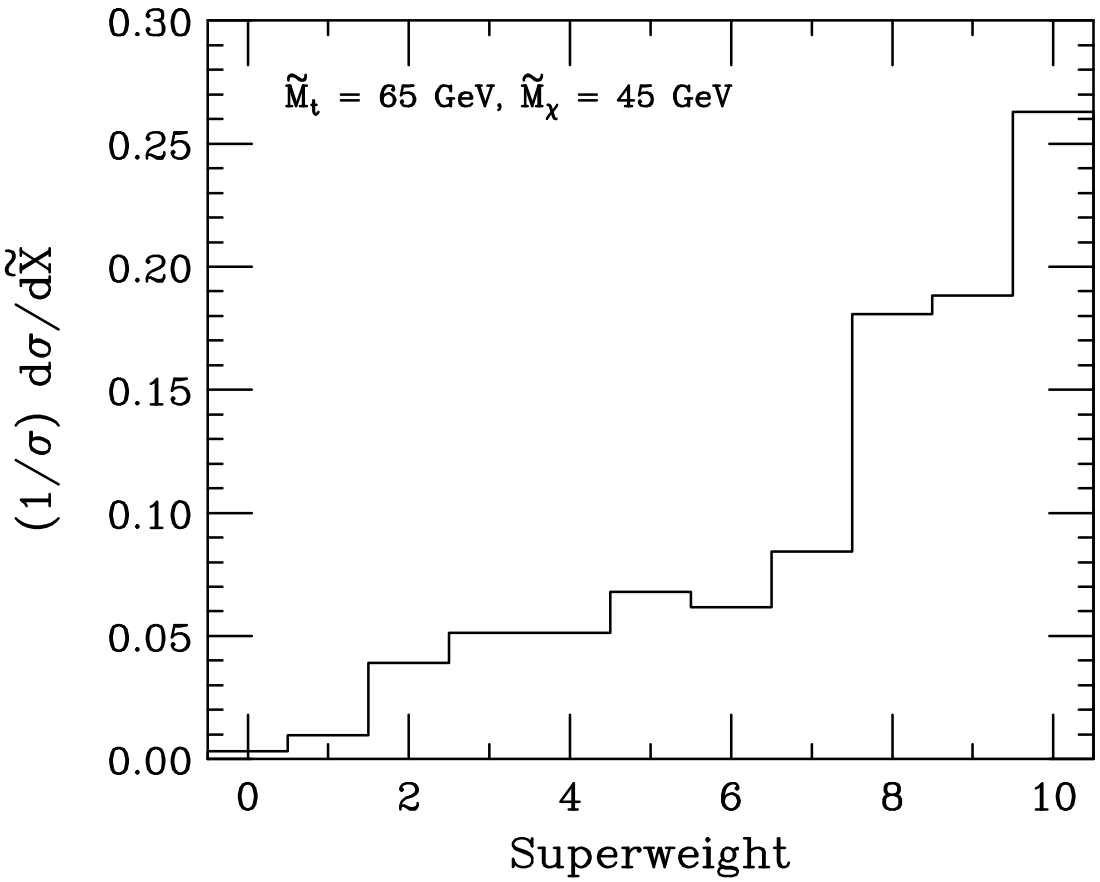

FIG. 7. Superweight distribution for $t\bar{t} \to cN_1N_1\bar{b}\ell^+\bar{\nu}_\ell$ events passing all of the cuts in Table I, for $\widetilde{M}_t = 65$ GeV, $\widetilde{M}_{N_1} = 45$ GeV. This histogram has been normalized to unit area.

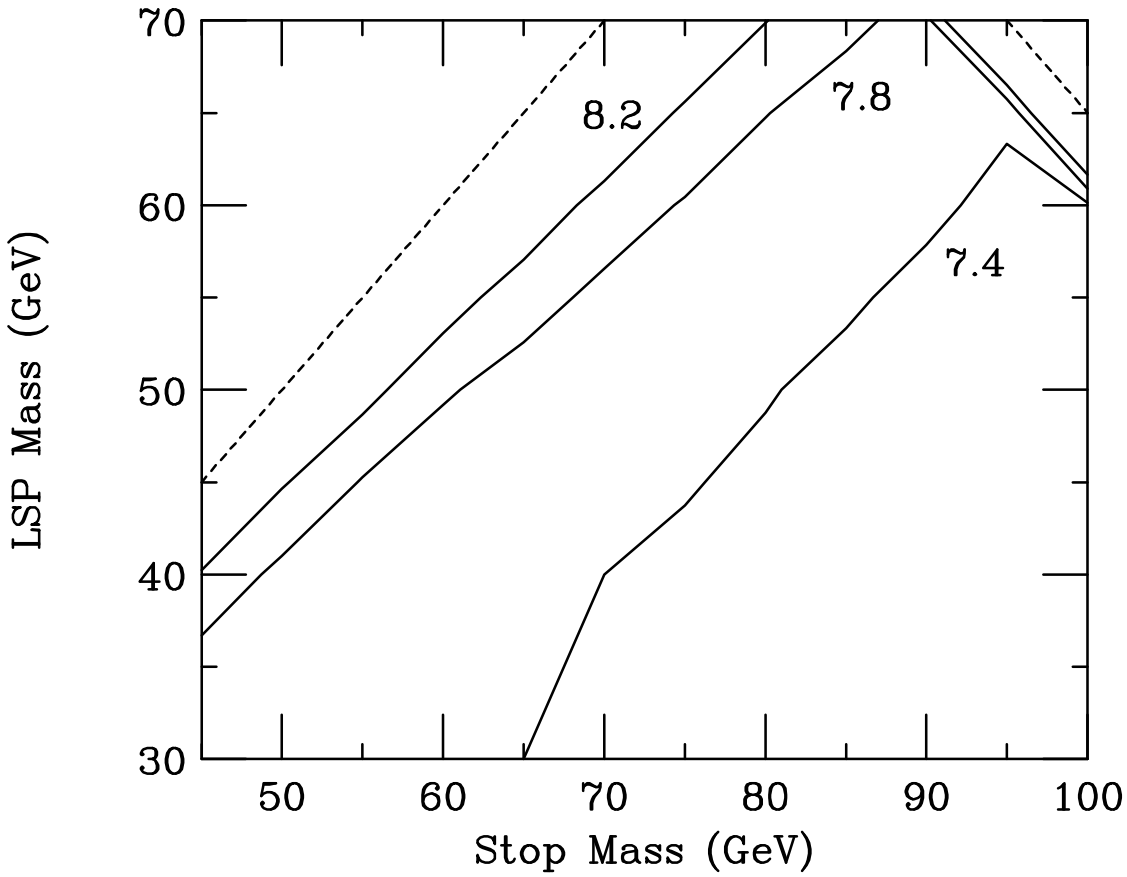

FIG. 8. Mean superweight for $t\bar{t} \to cN_1N_1\bar{b}\ell^+\bar{\nu}_\ell$ events passing all of the cuts in Table I, as a function of the stop and LSP masses. The kinematic limit is indicated by the dotted lines.

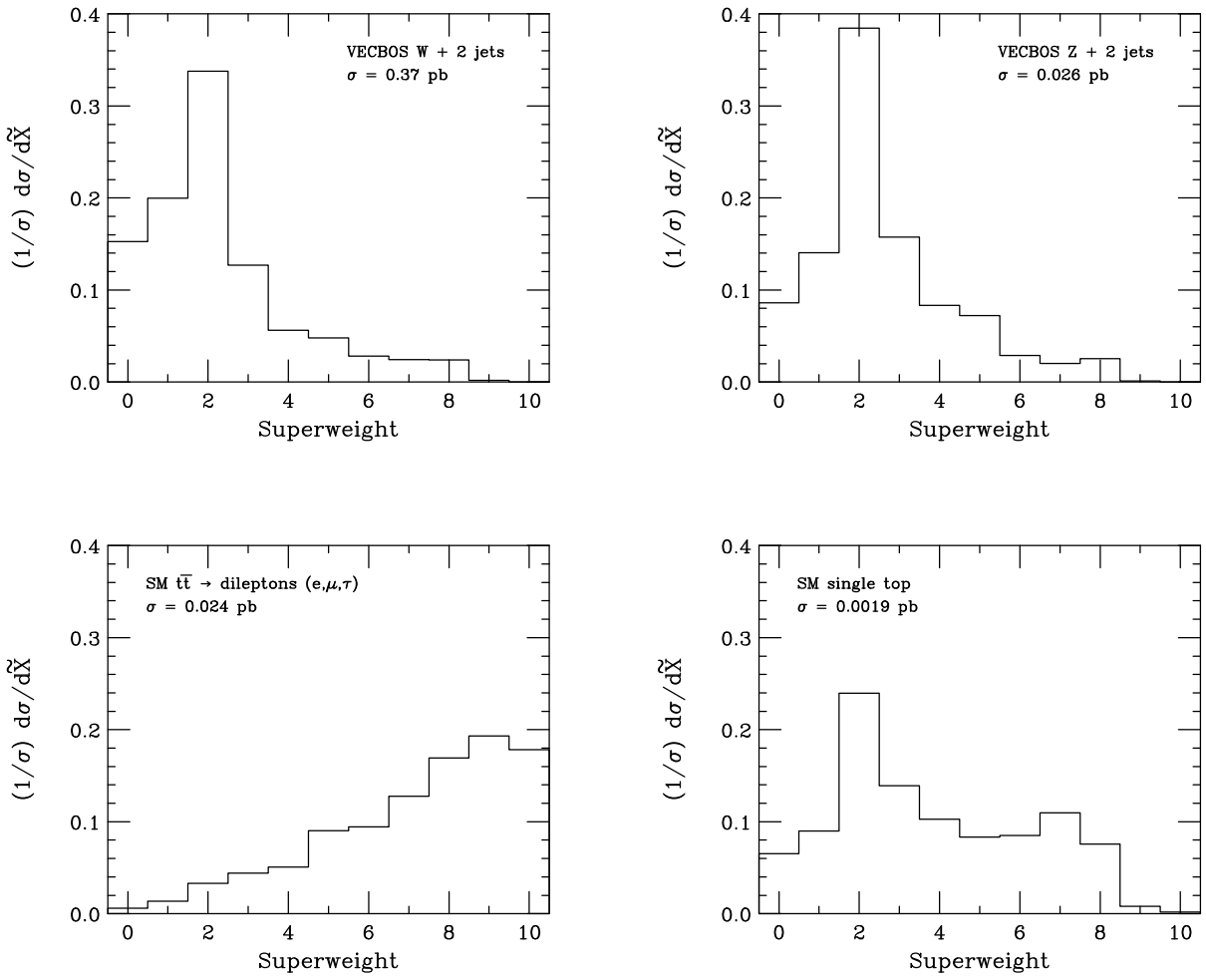

FIG. 9. Superweight distributions for background events passing all of the cuts in Table I. Each histogram has been normalized to unit area. Upper left: VECBOS $W + 2$ jets (88% of total). Upper right: VECBOS $Z + 2$ jets (6% of total). Lower left: $t\bar{t} \to$ dileptons, all combinations (6% of total). Lower right: single top production (<1% of total).

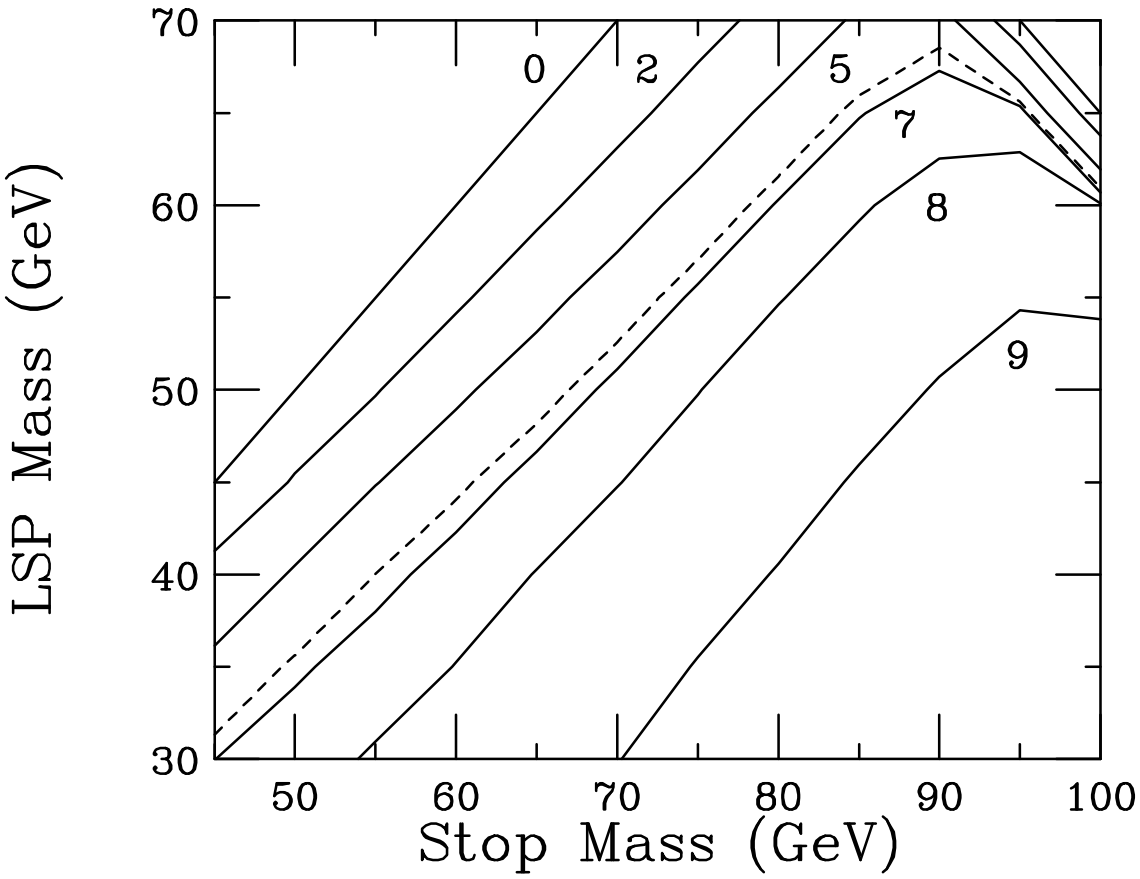

FIG. 10. Predicted number of $t\bar{t} \to cN_1N_1\bar{b}\ell^+\bar{\nu}_\ell$ events in 100 pb^{-1} passing all of the cuts in Table I, and satisfying the condition $\widetilde{\mathcal{X}} \geq 6$, as a function of the stop and LSP masses. Zero events are predicted at the kinematic limit. No K factor is included: see the discussion at the beginning of Sec. IV. Table VI indicates that 4.9 background events are expected for this choice. The dashed contour marks the point at which $S/\sqrt{B} = 3$.

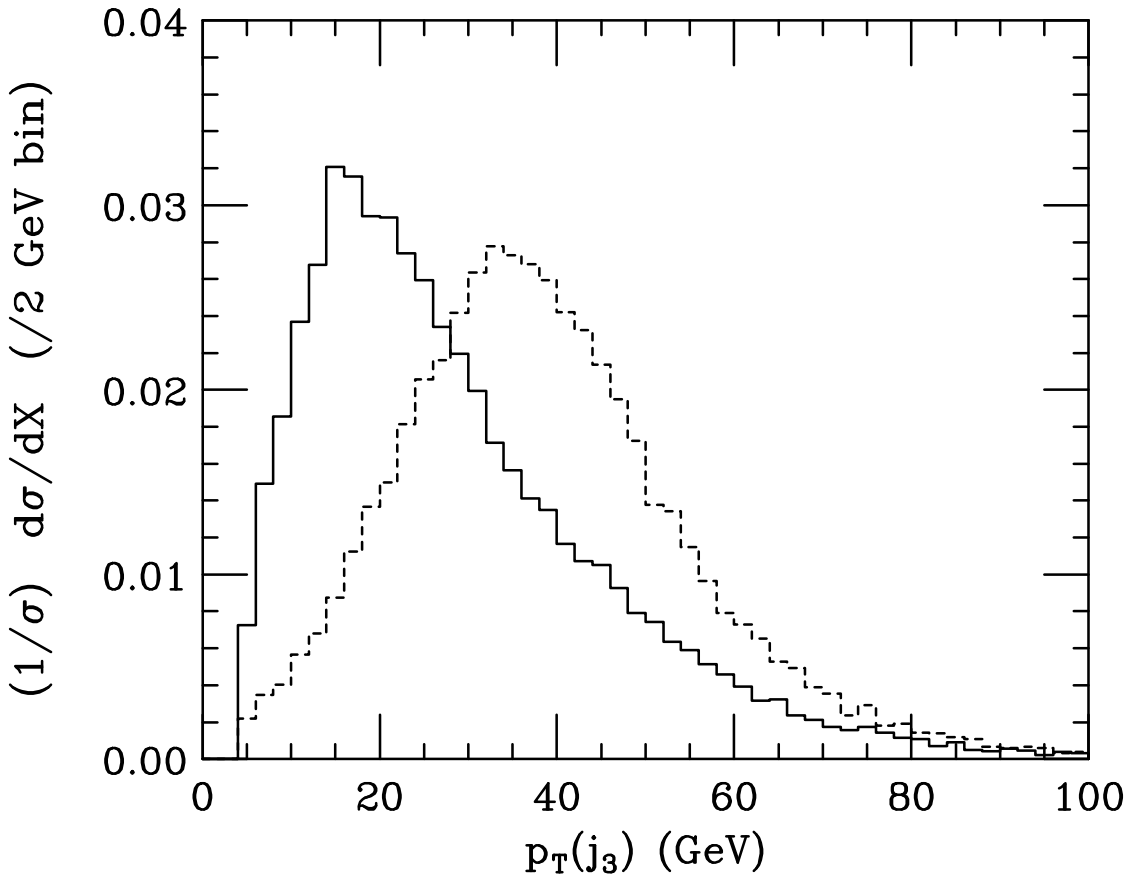

FIG. 11. Transverse momentum distributions of the jet with the third highest p_T (j_3) for $\tilde{g}\tilde{g}$, $\tilde{q}\tilde{q}$, and $\tilde{q}\tilde{g}$ production in the SUSY model summarized in Table VII (solid), and Standard Model $t\bar{t} \to W + 4$ jets (dashed). Only events which pass all of the cuts in Table I (except for the cut on $p_T(j_3)$) are included. A minimum reconstructed jet energy of 5 GeV is required. Both histograms have been normalized to unit area.

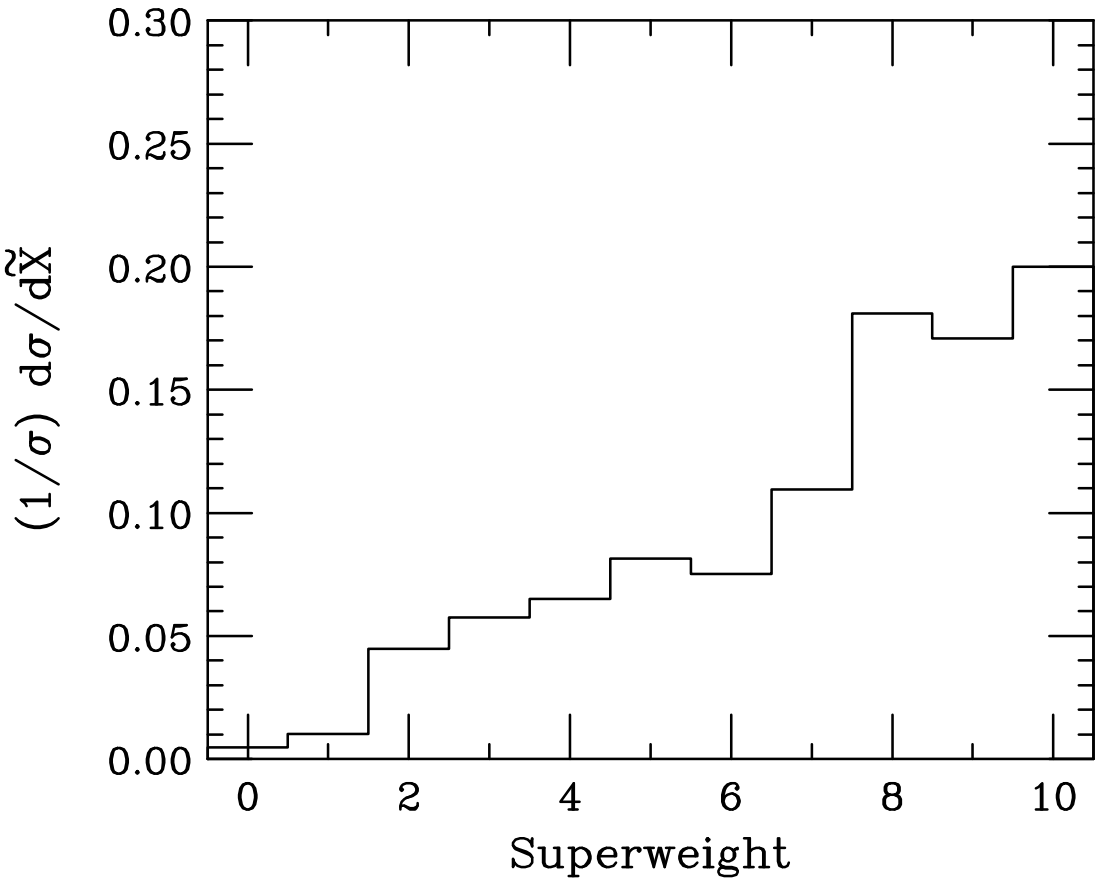

FIG. 12. Superweight distribution for N_1-containing $t\bar{t}$, $\tilde{g}\tilde{g}$, $\tilde{q}\tilde{q}$ and $\tilde{g}\tilde{q}$ events in the SUSY model summarized in Table VII which pass all of the cuts in Table I, but with a loosened requirement on the third jet, $p_T(j_3) < 30$ GeV. This histogram has been normalized to unit area.

TABLES

TABLE I. Cuts used for the $t \to \tilde{t}N_1$ search. We use the notation j for any of the reconstructed jets, j_h for either of the two highest E_T jets, and j_s for any of the additional (soft) jets, if present. We refer to the entries above the dividing line as the "basic" cuts.

$p_T(\ell) > 20$ GeV
$\not{p}_T > 20$ GeV
$p_T(j_h) > 15$ GeV
$p_T(j_s) < 10$ GeV
$\lvert\eta(\ell)\rvert < 1$
$\lvert\eta(j_h)\rvert < 2$
$\Delta R(j,j) > 0.4$
$\Delta R(j,\ell) > 0.4$
$m_T(\ell,\, \not{p}_T) > 100$ GeV

TABLE II. Largest backgrounds for the $t \to \tilde{t}N_1$ search in picobarns surviving the cuts listed in Table I. The values in column I (II) include (exclude) the cut on m_T.

Background	I	II
W + 2 jets	39.1	0.37
Z + 2 jets	0.24	0.026
W/Z ($\to \tau\nu/\tau\tau$) + jets	2.97	<0.0003
$t\bar{t}\to$ dileptons (ee, $e\mu$, $\mu\mu$)[a]	0.014	0.0054
$t\bar{t}\to$ dileptons ($e\tau$, $\mu\tau$, $\tau\tau$)[a]	0.040	0.018
$t\bar{t}\to W$ + 4 jets[a]	0.0058	0.00017
single top[a]	0.10	0.0019

[a]All top backgrounds assume the absence of non-SM production, and utilize $\mathcal{B}(t \to Wb) = 100\%$.

TABLE III. Cross section times branching ratios in picobarns and efficiency for signal events surviving the cuts listed in Table I for representative values of $\widetilde{M}_t$ and $\widetilde{M}_{N_1}$ in GeV. The values in column I (II) include (exclude) the cut on m_T. The quoted values assume $\mathcal{B}(t \to \tilde{t}N_1) = 50\%$. We do not include a K-factor for radiative corrections: see the beginning of Sec. IV.

$\widetilde{M}_t$	$\widetilde{M}_{N_1}$	I	II
60	50	0.10 (18%)	0.057 (10%)
60	45	0.16 (28%)	0.082 (14%)
60	35	0.21 (38%)	0.10 (18%)
65	45	0.19 (33%)	0.095 (17%)
65	35	0.23 (40%)	0.11 (19%)
75	45	0.23 (40%)	0.11 (19%)
85	50	0.24 (42%)	0.12 (20%)
95	60	0.23 (41%)	0.11 (20%)

TABLE IV. Superweight criteria for $t \to \tilde{t}N_1$ search. One unit is added to the superweight for a given event for each of the conditions on this list which are satisfied. Jet 1 refers to the highest p_T jet in the event, and jet 2 to the next-to-highest p_T jet. The entries are approximately ordered from most to least effective.

Criterion	Quantity	Condition
$\mathcal{C}_1$	missing transverse momentum	$\not{p}_T > 65$ GeV
$\mathcal{C}_2$	scalar sum of jet 2 and missing p_T	$p_T(j_2) + \not{p}_T > 95$ GeV
$\mathcal{C}_3$	difference in missing p_T and lepton p_T	$\not{p}_T - p_T(\ell) > 0$ GeV
$\mathcal{C}_4$	"W" transverse mass	$m_T(\ell, \not{p}_T) > 125$ GeV
$\mathcal{C}_5$	j_1-ℓ azimuthal angle	$\varphi_{j_1,\ell} < 2.4$ radians
$\mathcal{C}_6$	scalar sum of charged lepton and missing p_T	$p_T(\ell) + \not{p}_T > 150$ GeV
$\mathcal{C}_7$	scalar sum of jet 1 and missing p_T	$p_T(j_1) + \not{p}_T > 130$ GeV
$\mathcal{C}_8$	j_1-ℓ opening angle	$\cos\theta_{j_1,\ell} > -0.15$
$\mathcal{C}_9$	j_1-ℓ transverse mass	$m_T(j_1, \ell) < 125$ GeV
$\mathcal{C}_{10}$	visible mass	$m(\ell, j_1, j_2) < 200$ GeV

TABLE V. Superweight data for signal events surviving all of the cuts listed in Table I for representative values of $\widetilde{M}_t$ and $\widetilde{M}_{N_1}$ in GeV. For each pair of values we list the mean value of the superweight, the expected number of events in 100 pb^{-1} (based upon the entries in Table III), the expected number of events with a superweight of 6 (7,8) or greater in 100 pb^{-1}. No K factor is included: see the discussion at the beginning of Sec. IV.

$\widetilde{M}_t$	$\widetilde{M}_{N_1}$	$\langle\widetilde{\mathcal{X}}\rangle$	$N(\widetilde{\mathcal{X}} \geq 0)$	$N(\widetilde{\mathcal{X}} \geq 6)$	$N(\widetilde{\mathcal{X}} \geq 7)$	$N(\widetilde{\mathcal{X}} \geq 8)$
60	50	7.8	5.7	4.6	4.3	3.9
60	45	7.6	8.2	6.4	5.9	5.3
60	35	7.4	10.4	8.0	7.4	6.4
65	45	7.5	9.5	7.4	6.8	6.0
65	35	7.4	11.0	8.4	7.7	6.7
75	45	7.4	11.0	8.5	7.7	6.7
85	50	7.4	11.5	8.8	8.0	7.0
95	60	7.4	11.2	8.6	7.9	6.8

TABLE VI. Superweight data for background events surviving the cuts listed in Table I. Only those sources with an expected contribution of 0.001 pb or greater are listed. For events in each category we list the mean value of the superweight, the number of events expected in 100 pb^{-1} (based upon the entries in Table II), the number of events with a superweight of 6 (7,8) or greater in 100 pb^{-1}. The bottom line gives the totals, or weighted average, as appropriate.

Background	$\langle\widetilde{\mathcal{X}}\rangle$	$N(\widetilde{\mathcal{X}} \geq 0)$	$N(\widetilde{\mathcal{X}} \geq 6)$	$N(\widetilde{\mathcal{X}} \geq 7)$	$N(\widetilde{\mathcal{X}} \geq 8)$
W + 2 jets	2.3	36.5	2.9	1.8	1.0
Z + 2 jets	2.6	2.6	0.2	0.1	<0.1
$t\bar{t}\rightarrow$ dileptons (ee, $e\mu$, $\mu\mu$)[a]	7.1	0.5	0.4	0.3	0.3
$t\bar{t}\rightarrow$ dileptons ($e\tau$, $\mu\tau$, $\tau\tau$)[a]	7.2	1.8	1.4	1.2	1.0
single top[a]	3.8	0.2	<0.1	<0.1	<0.1
Combined	2.6	41.6	4.9	3.6	2.3

[a]All top backgrounds assume the absence of non-SM production, and utilize $\mathcal{B}(t \rightarrow Wb) = 100\%$.

TABLE VII. Masses and principle branching ratios for a SUSY model representative of the scenario discussed in Sec. II. The input parameters are $M_1 = 75$, $M_2 = 85$, $M_3 = 200$, $\mu = -45$ (all in GeV), and $\tan\beta = 1.1$. The light stop squark eigenstate has a mass of 65 GeV and $\mathcal{B}(\tilde{t} \to N_1\, c) = 1$. The heavy stop squark eigenstate as well as both sbottom squarks have large masses. The slepton masses in GeV are: $\widetilde{M}_{e_L} = 115$, $\widetilde{M}_{e_R} = 125$, and $\widetilde{M}_{\nu} = 112$. The symbol q is used collectively for the u, d, s, c, b quarks.

particle	mass	width	decay modes	B.R.
t	163 GeV	2.3 GeV	$t \to W^+ b$	52%
			$t \to N_1\, \tilde{t}$	33%
			$t \to N_3\, \tilde{t}$	12%
			$t \to N_2\, \tilde{t}$	3%
$\tilde{g}$	233 GeV	1.5 GeV	$\tilde{g} \to \tilde{t}^+\, \bar{t}$	50%
			$\tilde{g} \to \tilde{t}^-\, t$	50%
$\tilde{u}_L, \tilde{c}_L$	259 GeV	2.9 GeV	$\tilde{u}_L \to C_i^+\, d$	49%
			$\tilde{u}_L \to N_i\, u$	26%
			$\tilde{u}_L \to \tilde{g}\, u$	24%
$\tilde{d}_L, \tilde{s}_L$	261 GeV	2.8 GeV	$\tilde{d}_L \to C_i^-\, u$	48%
			$\tilde{d}_L \to \tilde{g}\, d$	27%
			$\tilde{d}_L \to N_i\, d$	25%
$\tilde{u}_R, \tilde{c}_R$	260 GeV	1.2 GeV	$\tilde{u}_R \to \tilde{g}\, u$	61%
			$\tilde{u}_R \to N_i\, u$	39%
$\tilde{d}_R, \tilde{s}_R$	260 GeV	1.2 GeV	$\tilde{d}_R \to \tilde{g}\, d$	86%
			$\tilde{d}_R \to N_i\, d$	14%
N_1	45 GeV		STABLE	
N_2	77 GeV	0.6 keV	$N_2 \to N_1\, \gamma$	82%

			$N_2 \to N_1\, q\, \bar{q}$	12%
N_3	93 GeV	0.11 MeV	$N_3 \to N_1\, q\, \bar{q}$	69%
			$N_3 \to N_1\, \nu\, \bar{\nu}$	21%
			$N_3 \to N_1\, \ell\, \bar{\ell}$	10%
C_1^+	83 GeV	0.41 GeV	$C_1^+ \to \tilde{t}^+\, \bar{b}$	100%
C_2^+	124 GeV	0.96 GeV	$C_2^+ \to \tilde{t}^+\, \bar{b}$	93%

TABLE VIII. Number of events in 100 pb^{-1} predicted to pass the cuts in Table I as a function of the cut on the third jet, within the context of the SUSY model described in Table VII. We break SM-produced $t\bar{t}$ events into signal and background contributions depending on whether or not there is a pair of N_1's in the final state. The third line contains the contributions from all squark and gluino events, whether or not any top appeared in the intermediate states. For comparison, we list the expected number of events in the absence of SUSY in the last line. No K factor is included: see the discussion at the beginning of Sec. V. The W/Z + jets background under these conditions is estimated to be an additional 39.1 events.

	$p_T(j_3) < 10$ GeV	$p_T(j_3) < 20$ GeV	$p_T(j_3) < 30$ GeV	$p_T(j_3) < \infty$
$t\bar{t}$ (background)	0.9	1.4	2.2	3.7
$t\bar{t}$ (signal)	7.9	9.4	9.8	10.3
$\tilde{g}\tilde{g}$, $\tilde{q}\tilde{q}$, $\tilde{g}\tilde{q}$	0.7	2.5	4.1	6.4
total signal	8.7	11.8	14.0	16.7
$t\bar{t}$ (SM only)	3.2	5.0	7.3	13.9

TABLE IX. Same as Table VIII, but with the additional requirement $\widetilde{\mathcal{X}} \geq 6$. The W/Z + jets background under these conditions is estimated to be an additional 3.1 events.

	$p_T(j_3) < 10$ GeV	$p_T(j_3) < 20$ GeV	$p_T(j_3) < 30$ GeV	$p_T(j_3) < \infty$
$t\bar{t}$ (background)	0.6	0.9	1.2	1.9
$t\bar{t}$ (signal)	5.8	6.9	7.1	7.4
$\tilde{g}\tilde{g}$, $\tilde{q}\tilde{q}$, $\tilde{g}\tilde{q}$	0.6	1.9	3.1	4.9
total signal	6.5	8.6	10.3	12.5
$t\bar{t}$ (SM only)	2.1	3.1	4.1	6.9